University of Groningen

University of Groningen

Axisymmetric liquid sloshing under low-gravity conditions

Veldman, Arthur

Published in:
Default journal

IMPORTANT NOTE: You are advised to consult the publisher's version (publisher's PDF) if you wish to cite from it. Please check the document version below.

Document Version
Publisher's PDF, also known as Version of record

Publication date:
1984

[Link to publication in University of Groningen/UMCG research database](#)

AXISYMMETRIC LIQUID SLOSHING UNDER LOW-GRAVITY CONDITIONS†

A. E. P. VELDMAN and M. E. S. VOGELS

National Aerospace Laboratory (NLR), P.O. Box 90502, 1006 BM Amsterdam, The Netherlands

Abstract—A numerical simulation program has been developed for the determination of dynamic liquid behaviour in partially filled cylindrical containers during weightlessness. The program, based on the unsteady Navier–Stokes equations, is capable to treat axisymmetric flow; arbitrary free-surface shapes are allowed. In the paper some examples are presented showing liquid response to rotation and axial vibration. The numerical simulations provide information which is used in the definition and evaluation of an experiment onboard Spacelab. The combined theoretical/experimental investigation is directed towards a more efficient design of attitude control systems.

1. INTRODUCTION

In response to a call for proposal for experiments to be executed during the first flight of Spacelab, the National Aerospace Laboratory (NLR) submitted an experimental program. Its general objective is to obtain information about characteristics of weightless dynamic systems which are partially liquid; in particular systems which feature a free liquid surface. A section of this program dealing with fluid dynamics is scheduled to be executed in Spacelab 1. These experiments will make use of partially filled containers which are subjected to prescribed motions[1].

The main purpose of the experiments is to obtain a better understanding of the behaviour of (sometimes large) amounts of liquid (fuel, coolant) which are present onboard spacecraft. This knowledge can be used, for instance, for a more efficient design of attitude control systems. As a secondary objective, the experiments will enlarge our knowledge of terrestrial systems in which capillary forces play an important role.

For a deeper insight into the phenomena which are going to be observed onboard Spacelab, the experiments are supported by a theoretical investigation. Some results of this theoretical investigation concerning two-dimensional planar sloshing have already been reported by Veldman[2]. In the paper an extension to axisymmetric sloshing will be presented.

The global behaviour of systems with a free liquid surface under weightless conditions differs markedly from the behaviour in a terrestrial environment. Presence of gravitation considerably simplifies the description of the problem, since in the majority of cases we may assume a flat free surface and treat fluid effects by small perturbation methods[3]. Under weightless conditions even the calculation of an equilibrium free-surface shape (no liquid motion) requires

an elaborate study. Of the many theoretical contributions to this subject we will only mention the comprehensive investigations of Concus and Finn[4], and the recent work of Siekmann *et al.*[5].

In the unsteady case, linearization techniques around an equilibrium position, as discussed above, can yield information about stability or instability of the equilibrium and about resonance frequencies. A survey of this aspect of the dynamic behaviour of liquids can be found in [3]. For the corresponding behaviour under low-gravity conditions, in which we are interested, we refer to the work of Reynolds and his collaborators (see [6], and the references therein) and to Schilling and Siekmann[7].

A review of techniques that can be used to calculate the dynamic behaviour of the complete (nonlinear) unsteady problem has been given by Ousset[8] and Guibert *et al.*[9]. They point out that the most reliable results are to be expected from the solution of the complete Navier–Stokes equations. In this paper we will describe a numerical method with which the Navier–Stokes equations can be solved. The method is an extension of the SOLA–VOF method[10], a recent member of the Marker-and-Cell family. A number of examples showing the capabilities of the method is presented.

2. MATHEMATICAL DESCRIPTION

Our interest lies in the simulation of particular types of liquid motion, such as flows in which nonlinear effects can play an important role, or flows which are induced by viscous effects (e.g. spin-up). Therefore we have chosen the unsteady Navier–Stokes equations to describe the liquid dynamics. The equations of motion will be formulated in primitive variables (i.e. velocity and pressure); this facilitates the implementation of the free-surface boundary condition for the pressure. As a (non-essential) simplification it is assumed that the flow is laminar, and that the liquid is incompressible with constant material properties such as viscosity, surface tension and contact angle.

It is convenient to formulate the equations of motion in a reference frame which is fixed to the container (which may be moving with respect to an inertial reference frame). In such a container-fixed frame the flow equation can be written as:

conservation of mass

$$\text{div } \mathbf{u} = 0, \tag{1a}$$

conservation of momentum

$$\frac{D}{Dt}\mathbf{u} = -\text{grad } \bar{p} + v \text{ div grad } \mathbf{u} + \mathbf{F}. \tag{1b}$$

The following symbols have been introduced

u   velocity in the container-fixed frame
$\bar{p}$ normalized pressure, $\bar{p} = p/\rho$ (p: pressure, ρ: density)
v kinematic viscosity
F   virtual body force due to the motion of the container

$$\mathbf{F} = -\frac{d}{dt}\mathbf{q}_o - \Omega \times \mathbf{q}_o - 2\Omega \times \mathbf{u} - \frac{d}{dt}\Omega \times \mathbf{r}$$
$$-\Omega \times (\Omega \times \mathbf{r})$$

$\mathbf{q}_o$ velocity of a point O of the container with respect to an inertial frame
Ω angular velocity of the container
$\mathbf{r}$ radius vector pointing away from O
D/Dt   Lagrangian time derivative

These equations have to be supplied with a set of boundary conditions. At the container wall a no-slip condition applies

$$\mathbf{u} = \mathbf{0}.$$

At the free surface the stresses must be continuous. Assuming that the gas or vapor outside the liquid is not able to resist tangential stresses, and setting the external pressure at zero, we have[11]:

$$-\bar{p}n_i + v\left(\frac{\partial u_i}{\partial n_j} + \frac{\partial u_j}{\partial n_i}\right)n_j = 2\bar{\sigma}Hn_i \, (i = 1, 2, 3). \tag{2}$$

Here

n   normal at liquid surface pointing away from the liquid
$\bar{\sigma}$ kinematic surface tension, $\bar{\sigma} = \sigma/\rho$
H mean curvature of the free surface.

Further, when the free surface intersects the container wall a contact angle θ must be present.

Finally initial conditions must be specified which prescribe at $t = 0$ the velocity field and the position of the free surface.

With the above model axisymmetric flow has been studied in cylindrical containers (Fig. 1). This allows
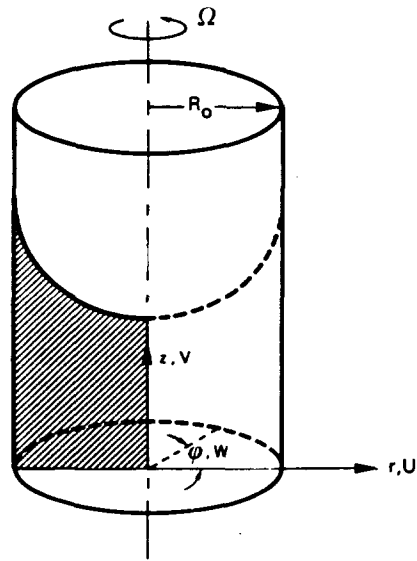

Fig. 1. Cylinder, coordinates and notation.

introduction of a cylindrical coordinate system (r, φ, z). Making use of the axial symmetry the equations of motion become:

$$\frac{\partial u}{\partial r} + \frac{u}{r} + \frac{\partial v}{\partial z} = 0,$$

$$\frac{\partial u}{\partial t} + u\frac{\partial u}{\partial r} + v\frac{\partial u}{\partial z} - \frac{1}{r}(w + \Omega r)^2$$
$$= -\frac{\partial \bar{p}}{\partial r} + v\left[\frac{\partial^2 u}{\partial r^2} + \frac{1}{r}\frac{\partial u}{\partial r} - \frac{u}{r^2} + \frac{\partial^2 u}{\partial z^2}\right],$$

$$\frac{\partial w}{\partial t} + u\frac{\partial w}{\partial r} + v\frac{\partial w}{\partial z} + \frac{uw}{r} + 2u\Omega + r\frac{d\Omega}{dt}$$
$$= v\left[\frac{\partial^2 w}{\partial r^2} + \frac{1}{r}\frac{\partial w}{\partial r} - \frac{w}{r^2} + \frac{\partial^2 w}{\partial z^2}\right],$$

$$\frac{\partial v}{\partial t} + u\frac{\partial v}{\partial r} + v\frac{\partial v}{\partial z} + \frac{dq_0}{dt}$$
$$= -\frac{\partial \bar{p}}{\partial z} + v\left[\frac{\partial^2 v}{\partial r^2} + \frac{1}{r}\frac{\partial v}{\partial r} + \frac{\partial^2 v}{\partial z^2}\right].$$

Here u, w and v are the velocity components in $r-$, $\varphi-$ and z-direction respectively; $\Omega = \Omega\mathbf{i}_z$ and $\mathbf{q}_0 = q_0\mathbf{i}_z$.

3. NUMERICAL METHOD

Since its introduction in the mid-sixties[12] the Marker-and-Cell method has become one of the most popular methods for calculating free-surface flows. Several versions have been developed, each one dedicated to specific physical situations. In the present investigation a version is required which is able to treat arbitrary free-surface shapes and which can treat capillary effects (surface tension). Such a method has been introduced recently by Hirt and Nichols[10]; it is called SOLA-VOF.

The special feature of the SOLA–VOF method is the volume-of-fluid (VOF) technique for keeping track of the location of the fluid and in particular its free surface. In the VOF technique a function F is defined which indicates the fractional volume occupied by the fluid in a grid cell. Thus a unit value of F indicates the cell is full of fluid, whereas a zero value indicates an empty cell. Cells with F values between zero and one must then contain a free surface. Surface locations, slopes and curvatures are easily computed, and the F distribution can be advanced in time by advection $(DF/Dt = 0)$. Some care has to be taken, however, in order not to introduce too much smoothing of the free surface, and, on the other hand, not to introduce instabilities. For a detailed description of the advection algorithm we refer to[10].

Like most members of the Marker-and-Cell family the SOLA–VOF method is an explicit finite-difference method. It makes use of a rectangular grid which covers the computational domain; stretching of the grid is possible. The dependent variables are defined at staggered locations in the grid, as shown in Fig. 2. The momentum equations in r-, φ- and z-direction are applied at the points where the corresponding velocity components, u, w and v, respectively, are defined. We note that in the original SOLA–VOF method no azimuthal velocities are included ($w = 0$); the φ-momentum equation, however, is easily added.

For the spatial discretization of the viscous terms central differencing is used. The convective terms can be discretized by either upwind differencing or central differencing. In most applications we have adopted upwind differencing, as this allows use of a larger time step (see the remarks on stability below). However, its discretization error has the effect of adding viscosity to the fluid. This artificial viscosity may well dominate the real viscosity. Hence in flows where viscous effects play an important role care has to be taken in interpreting the results of the calculations. A comprehensive discussion of this subject has been given by Gresho and Lee[14].
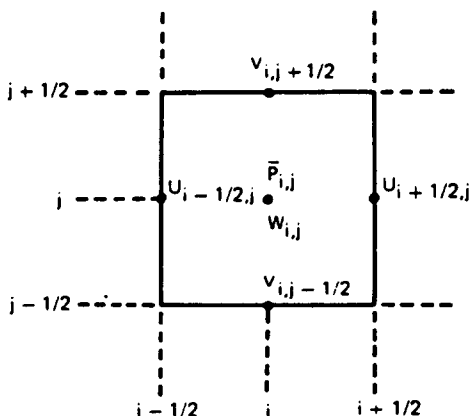
In temporal direction SOLA–VOF is an explicit, two-level method. The time derivative is descretized with first-order accuracy. A time step from $t^n = n\Delta t$ to $t^{n+1} = (n + 1)\Delta t$ is organized in the following way: Abbreviate the Navier–Stokes equations (1) as

$$\text{div } \mathbf{u} = 0,$$

$$\frac{\partial}{\partial t} \mathbf{u} + \text{grad } \bar{p} = \mathbf{R}, \tag{3}$$

then the discretization in time can be written as

$$\text{div } \mathbf{u}^{n+1} = 0, \tag{4a}$$

$$\frac{\mathbf{u}^{n+1} - \mathbf{u}^n}{\Delta t} + \text{grad } \bar{p}^{n+1} = \mathbf{R}^n. \tag{4b}$$

The subscript denotes the time level, e.g. $\mathbf{u}^n = \mathbf{u}(t^n)$. Taking the divergence of (4b) and using (4a) we obtain finally

$$\text{div grad } \bar{p}^{n+1} = \frac{1}{\Delta t} \text{div } (\mathbf{u}^n + \Delta t\,\mathbf{R}^n), \tag{5a}$$

$$\mathbf{u}^{n+1} = \mathbf{u}^n + \Delta t\,\mathbf{R}^n - \Delta t \text{ grad } \bar{p}^{n+1}. \tag{5b}$$

Equation (5a) is a Poisson equation for the pressure, to be solved in the domain occupied by the fluid. At the free surface, taken in its position at $t = t^n$, a Dirichlet condition applies

$$\bar{p}^{n+1} = -2\bar{\sigma}H^n,$$

where H^n is the mean curvature at time level t^n. This condition follows from the normal component of the stress relation (2) after neglect of the contribution of the viscous shear stress. At the container wall a boundary condition for $\bar{p}$ can be found by considering the normal component of (4b). This results in a Neumann condition

$$\frac{\partial}{\partial n} \bar{p}^{n+1} = \mathbf{n} \cdot \mathbf{R}^n,$$

where $\mathbf{n}$ is the normal to the container wall. The Poisson equation has been solved with an alternating line-relaxation technique. Some of our calculations have been performed on a Cyber 205; in these calculations point-relaxation has been used because the latter technique can be vectorized more efficiently. Both techniques are described in[14].

As in any explicit method the time step Δt is restricted by stability criteria. In general stability of the numerical process requires that (numerical) errors do not grow in time. It is very difficult for nonlinear equations to obtain precise (necessary and sufficient) stability criteria, but for practical purposes the fol-

Fig. 2. The arrangement of the variables in a grid cell.

lowing ones (based on linearized theory) are useful as a "rule-of-thumb" (see [2, 14, 15]):

$$\nu \Delta t \left\{ \frac{1}{(\Delta r)^2} + \frac{1}{(\Delta z)^2} \right\} \le \tfrac{1}{2},$$

$$\Delta t \max \left\{ \frac{|u|}{\Delta r}, \frac{|v|}{\Delta z} \right\} \le 1,$$

$$\bar{\sigma}(\Delta t)^2 \max \left\{ \frac{1}{(\Delta r)^3}, \frac{1}{(\Delta z)^3} \right\} \le \frac{4}{9\pi}.$$

The above conditions apply when upwind differencing is used for the convective terms. When central differencing is used an additional criterion has to be satisfied

$$\Delta t \max(u^2, v^2)/\nu \le 2.$$

For fluids with small viscosity the latter criterion usually is the most restrictive; the switch to upwind differencing is often made to avoid this criterion.

4. EXAMPLES OF CALCULATIONS

We will now illustrate the type of problems which can be analyzed with the method described above. Hereto we have performed some calculations for the cylindrical container to be used in the Spacelab experiment (see Fig. 1). It has radius 2.5 cm and height 8 cm. The container is partially filled with a silicon oil with kinematic surface tension $\bar{\sigma} = 20$ cm^3 sec^{-2} and kinematic viscosity $\nu = 0.03$ cm^2 sec^{-1}. The

contact angle of the liquid/solid combination is 0°; in the numerical simulations a value of 10° has been used.

Since axisymmetric motion is being studied, the computational domain is restricted to a meridional plane.

4.1 Rotating cylinder

In the first example we show a case in which the shape of the region occupied by the liquid (and hence the free surface) undergoes a large deformation. This case makes high demands upon the surface tracking mechanism; the calculations clearly demonstrate the power of the VOF method.

In this example the liquid motion is induced by increasing the rate of rotation around the axis of symmetry of the cylinder. At $t = 0$ the half-filled container is at rest; the fluid is situated at the lower part of the cylinder (see Fig. 3, $t = 0$) and dimensionless particles are spread with regular intervals over the fluid region.

Now the angular velocity is increased linearly from $\Omega = 0$ rpm at $t = 0$ to $\Omega = 35$ rpm at $t = 35$ sec. After 35 sec Ω is held at 35 rpm (see Fig. 4).

Figure 3 gives an impression of the spin-up process; the position of the free surface and of the particles is shown at various points of time. By making many pictures and taking a shot of each picture, a motion-picture is made which shows the spin-up in full detail. The first ten seconds show merely a movement of the particles. After that the fluid is forced up the outer wall. Shortly before $t = 40$ sec the fluid reaches the top and a bubble-like shape is found. This bubble eventually bulges out to an annular shape.
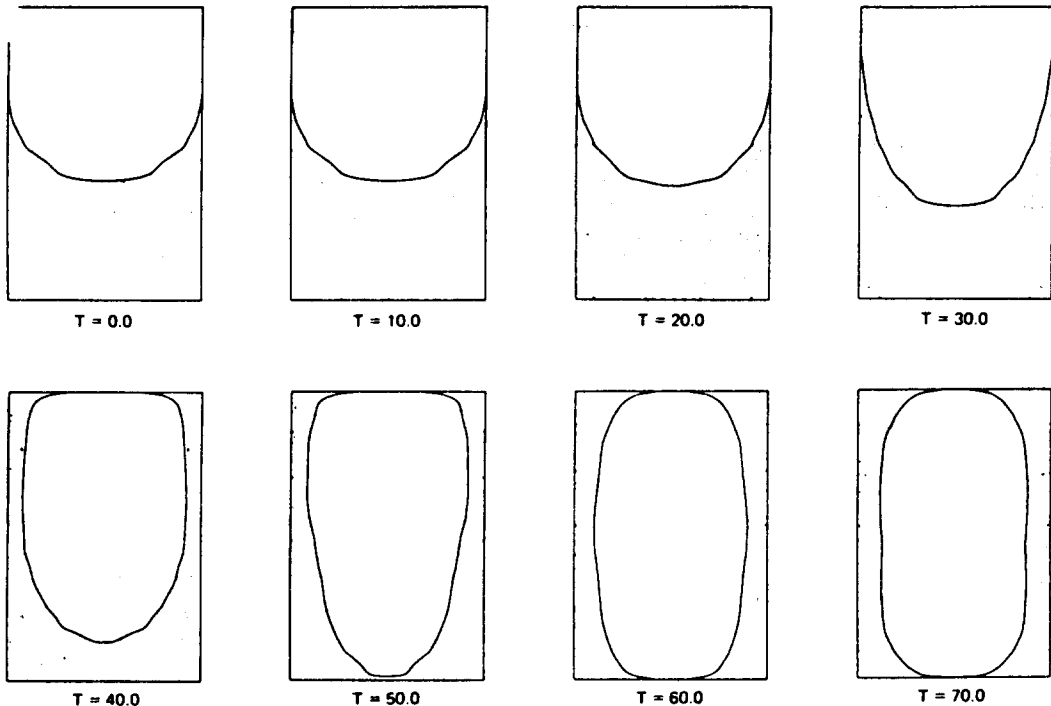

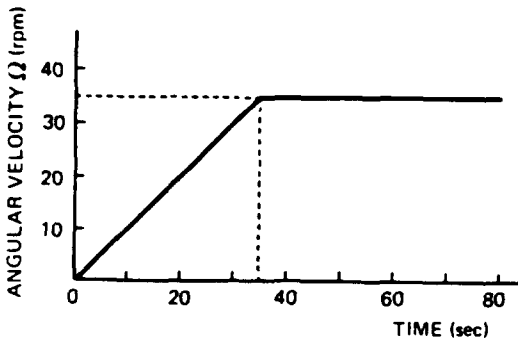Fig. 3. Dynamic response to spin-up from $\Omega = 0$ rpm to $\Omega = 35$ rpm.

Fig. 4. Angular velocity in spin-up example.

In order to be able to capture the thin layers that occur during the spin-up process the 8 × 16 grid was smoothly stretched with more points near the solid walls. The time step used was 0.002 sec. The calculation required about 10^{-2} CPU sec/time step on a CYBER 205.

4.2 Forced axial vibrations

In the second example we have used the present method to calculate the response to forced axial vibrations; it will be shown that the orientation of the free surface has a considerable influence on the response behaviour.

Schilling and Sieckmann[7] have analyzed a similar problem by a different method, but had to limit the impressed motion to small excitations of harmonical nature. Using the present method arbitrary excitations are allowed; nonlinear effects can be studied, as well as the transient response behaviour.

Calculations have been performed with a container which is half filled with liquid. The liquid is positioned in equilibrium in the lower half of the container. At $t = 0$ the container is set into an axial vibration with frequency ω and amplitude A, according to
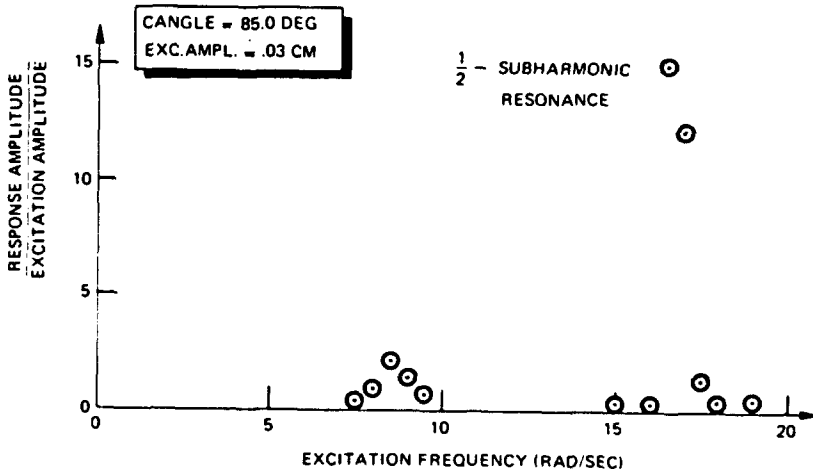
$$q_0(t) = -\omega A \cos(\omega t).$$

In this example the computational grid was chosen 6 × 12. Stretching in vertical direction was applied to obtain a higher resolution near the free surface; the vertical mesh spacing varied from 0.52 cm near the free surface to 0.91 cm near top and bottom of the container.

The timestep used was 0.01 sec. On a Cyber 73–28 computer a timestep on this grid requires about 0.4 CPU sec.

Two configurations have been investigated. The first one is chosen such that the free surface is about horizontal. This corresponds to terrestrial conditions where gravity dominates the capillary effects, but also to low-gravity conditions in combination with a contact angle near 90°. The calculations have been performed with $\theta = 85°$, since for $\theta = 90°$ the fluid remains in its initial equilibrium position. The results of the calculations can be compared with analytical results which are available for a horizontal free surface[16].

For a range of frequencies the liquid response between $t = 0$ and $t = 30$ sec has been computed. For most frequencies 30 sec appear to be long enough for the fluid to have attained a steady response. Figure 5 shows the steady response amplitude of the free-surface height at the axis as a function of the excitation frequency ω for a fixed excitation amplitude $A = 0.03$ cm. Linear theory based on a horizontal fluid surface predicts a lowest axisymmetric sloshing frequency ω_1 according to[16]

$$\omega_1^2 = \bar{\sigma}\left(\frac{3.8317}{R_0}\right)^3 \tanh\left(\frac{3.8317\,h}{R_0}\right), \quad (6)$$

where R_0 is the radius of the container and h the liquid height. The number 3.8317 corresponds to the first zero of the Bessel function J_1. For the present configuration ($R_0 = 2.5$ cm and $h = 4$ cm) eqn (6) yields a value $\omega_1 = 8.49$ rad/sec.

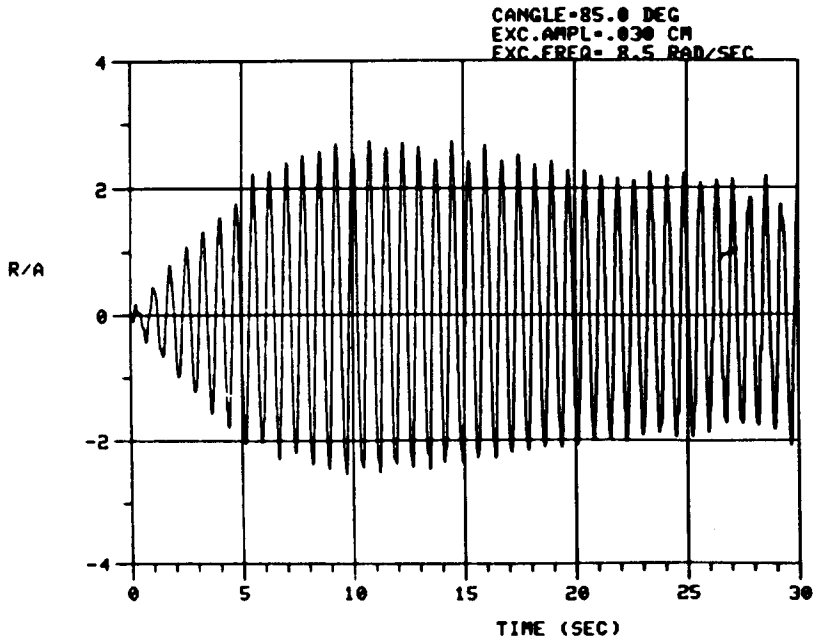Inspection of Fig. 5 reveals two peaks: one around $\omega = \omega_1$, corresponding to harmonic resonance at the

Fig. 5. Response of free surface to axial vibrations for $\theta = 85°$; note the $\frac{1}{2}$-subharmonic resonance.

Fig. 6. Transient response of free surface height to axial vibration at lowest eigenfrequency ($\theta = 85^{\circ}$).

eigenfrequency, and a much larger one around $\omega = 2\omega_1$. The latter peak corresponds to $\frac{1}{2}$-subharmonic resonance. Linear theory, featuring the Mathieu equation, can be used to predict the latter behaviour[16]. It is interesting to look at the time history of the resonance at the two peaks.

Figure 6 presents the motion of the axial free-surface height for $\omega = 8.5$ rad/sec; the figure shows

the response R (i.e. the deviation from the equilibrium position) divided by the excitation amplitude A. The fluid responds quickly in the excitation frequency ($\approx$ eigen-frequency). The situation is completely different when $\omega = 2\omega_1$.

Figure 7 shows the response at $\omega = 16.5$ rad/sec (corresponding to the largest response obtained). Now it takes about 30 sec for the fluid to reach a
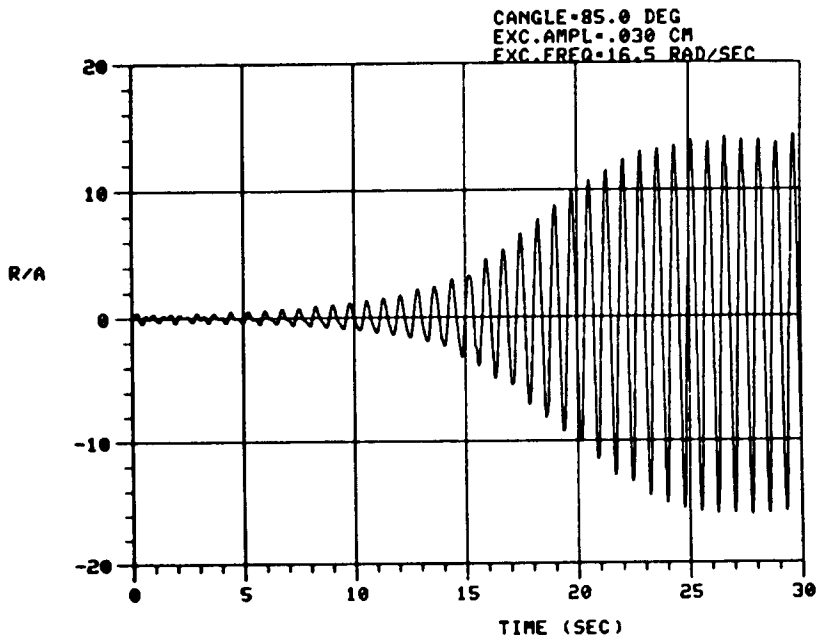

Fig. 7. Transient response of free surface height to axial vibration at twice the lowest eigenfrequency; $\frac{1}{2}$-subharmonic resonance ($\theta = 85^{\circ}$).
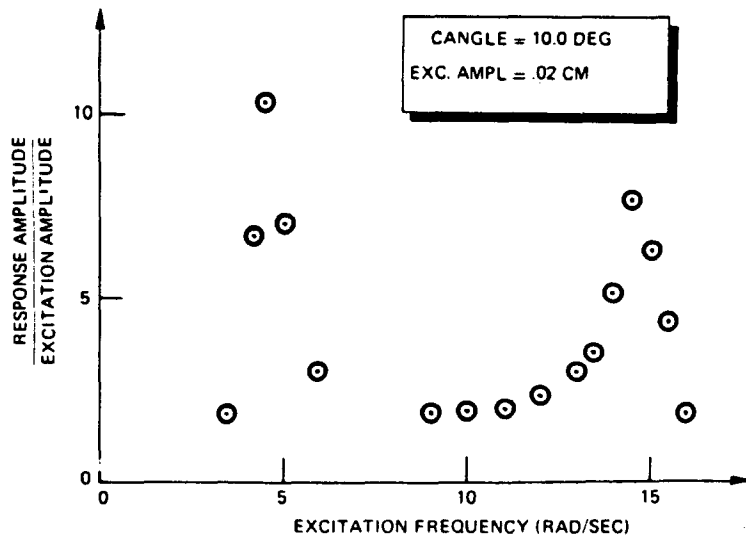
Fig. 8. Response of free surface to axial vibrations for $\theta = 10°$.

steady response. Moreover, whereas the fluid starts to respond in the excitation frequency, the final response is in the basic eigenfrequency.

The second configuration analyzed is typical for a low-gravity environment. For a contact angle $\theta = 0°$ the free-surface forms half of a sphere, and can no longer be considered horizontal. To our knowledge no analytical results are available for this configuration. Again we have been vibrating the container: excitation amplitude in this case $A = 0.02\,cm$. Figure 8 shows the steady response amplitude of the axial surface height as a function of ω. Two peaks are visible, one around $\omega = 4.5\,rad/sec$

and another one around $\omega = 14.5\,rad/sec$. As the fluid responds in the excitation frequency (Figs. 9 and 10) these peaks correspond to eigenfrequencies. Note that the lowest eigenfrequency has decreased as compared with the previous case with $\theta = 85°$. In contrast with the previous case no $\frac{1}{2}$-subharmonic resonance can be found in Fig. 8. Yet the response at $\omega = 9\,rad/sec$ (i.e. twice the lowest eigenfrequency) is worthwhile showing (Fig. 11). The fluid starts to respond in the lowest eigenfrequency ($\frac{1}{2}$-subharmonic), but gradually switches to the excitation frequency. Thus, the response is just the opposite of the behaviour shown in Fig. 7.
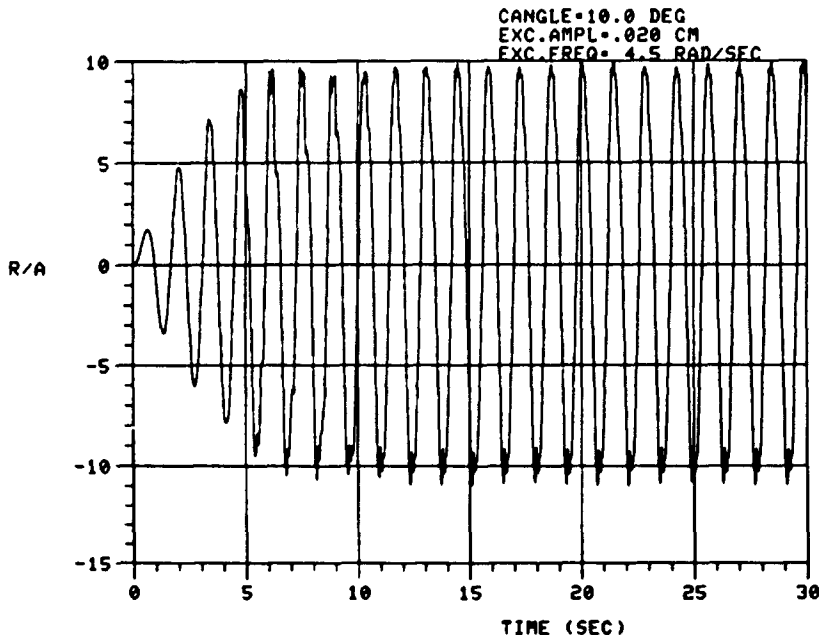

Fig. 9. Transient response of free surface height to axial vibration at lowest eigenfrequency ($\theta = 10°$).
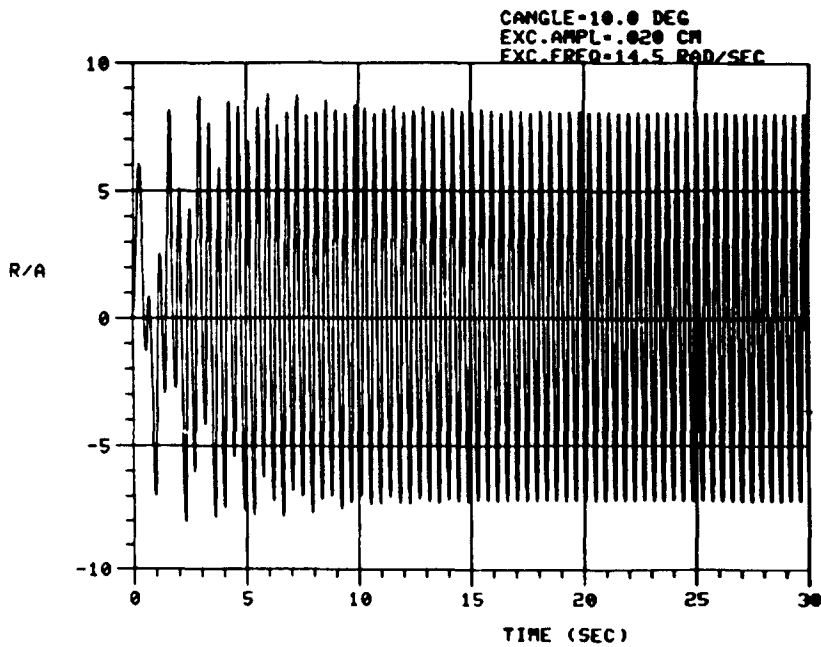
CANGLE=10.0 DEG
EXC.AMPL=.020 CM
EXC.FREQ=14.5 RAD/SEC

Fig. 10. Transient response of free surface height to axial vibration at second eigenfrequency ($\theta = 10°$).

For more information on these forced vibrations, including Fourier spectra of the response, we refer to[14].

5. CONCLUDING REMARKS

A numerical algorithm has been presented which can be used to simulate axisymmetric liquid sloshing under low-gravity conditions. The algorithm is an extension of the SOLA-VOF method. A low-gravity environment makes high demands on the surface-tracking mechanism since large deformations of the free surface will frequently occur; this in contrast with terrestrial conditions where gravity is dominating. The examples presented clearly demonstrate that the VOF technique is capable to follow the free surface during large deformations. This makes the method highly flexible with respect to liquid configurations which can be simulated.
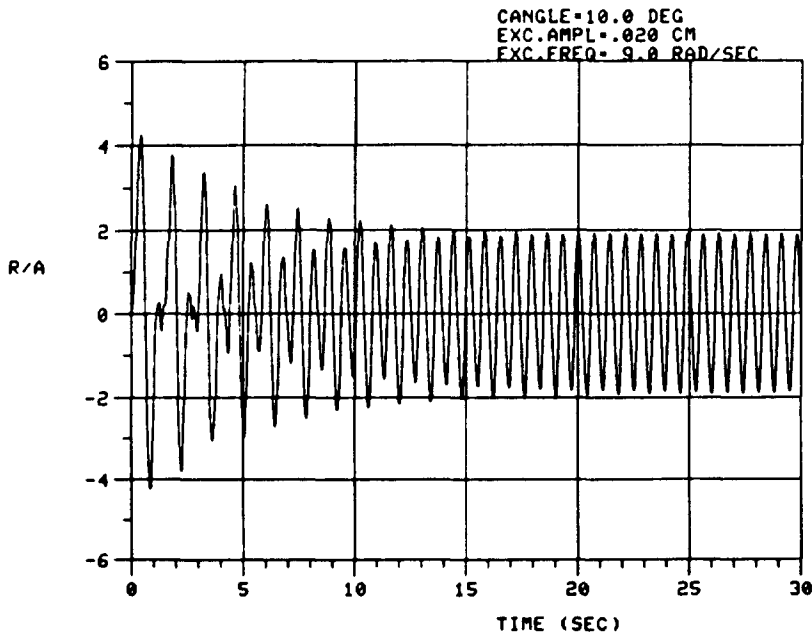
CANGLE=10.0 DEG
EXC.AMPL=.020 CM
EXC.FREQ= 9.0 RAD/SEC

Fig. 11. Transient response of free surface height to axial vibration at twice the lowest eigenfrequency ($\theta = 10°$).

Future developments include extension of the method to three-dimensional situations. Also, the mathematical model can be extended to describe the interaction between the liquid dynamics and the motion of the container. Thus a tool will become available with which the dynamic behaviour of free-floating liquid-filled containers can be predicted. Such a tool is applicable in the design of attitude control system for spacecraft carrying large amounts of liquid.

REFERENCES

1. J. P. B. Vreeburg. Spacelab experiments to study the coupling between liquid and solid motions in a 0-g environment. *NLR TR* 76097 L (1976).
2. A. E. P. Veldman. Liquid sloshing under low-g conditions: mathematical model and basic numerical method. *NLR TR* 79057 U (1979).
3. H. N. Abramson (Editor). *The Dynamic Behaviour of Liquids in Moving Containers.* NASA SP-106 (1966).
4. P. Concus and R. Finn. On capillary free surfaces in the absence of gravity. *Acta Math.* **132**, 177–198 (1974).
5. J. Siekmann, W. Scheideler and P. Tietze. Static meniscus configurations in propellant tanks under reduced gravity. *Comp. Meth. Appl. Mech. Engng.* **28**, 103–116 (1981).
6. W. C. Reynolds and H. M. Satterlee. Liquid propellant behaviour at low and zero g, *The Dynamic Behaviour of Liquids in Moving Containers*, Chap. 11. *NASA SP*-106 (1966).
7. U. Schilling and J. Siekmann. Numerical calculation of the translational forced oscillations of a sloshing liquid in axially symmetric tanks. *Collection of papers of the 24th Israel Annual Conf. on Aviation and Astronautics.* (Feb. 1982).
8. Y. Ousset. Etat actuel de la recherche sur la dynamique des fluides en rotation. *ESA J.* **1**, 43–70 and 189–208 (1977).
9. J. P. Guibert, H. T. Huynh, L. J. Marce, *et al.* Etude generale de l'influence des liquides contenus dans les satellites, Rapport 1/3307 SY, ONERA (1978).
10. C. W. Hirt and B. D. Nichols. Volume of Fluid (VOF) method for the dynamics of free boundaries. *J. Comput. Phys.* **39**, 201–225 (1981).
11. G. K. Batchelor, *An Introduction to Fluid Dynamics.* University Press, Cambridge (1970).
12. J. E. Welch, F. H. Harlow, J. P. Shannon and B. J. Daly. The MAC method: a computing technique for solving viscous, incompressible, transient fluid-flow problems involving free surfaces. Los Alamos Rep. *LA*-3425 (1966).
13. P. M. Gresho and R. L. Lee. Don't suppress the wiggles— they're telling you something! *Computers and Fluids* **9**, 223–253 (1981).
14. A. E. P. Veldman and M. E. S. Vogels. Liquid sloshing under low-g conditions II: axisymmetric motion, *NLR report,* to be published.
15. C. W. Hirt and J. L. Cook. Calculating three-dimensional flows around structures and over rough terrain. *J. Comput. Phys.* **10**, 324–340 (1972).
16. F. T. Dodge, D. D. Kana and H. N. Abramson. Liquid surface oscillations in longitudinally excited rigid cylindrical containers. *AIAA J.* **3**, 685–695 (1965).